

¹ Heterogeneous Nature of Relaxation Dynamics of Room-Temperature Ionic Liquids $(\text{EMIm})_2[\text{Co}(\text{NCS})_4]$ and $(\text{BMIm})_2[\text{Co}(\text{NCS})_4]$

³ Stella Hensel-Bielówka, ^{*,†} Żaneta Wojnarowska, [‡] Marzena Dzida, [†] Edward Zorębski, [†] Michał Zorębski, [†]
⁴ Monika Geppert-Rybczyńska, [†] Tim Peppel, [§] Katarzyna Grzybowska, [‡] Yangyang Wang, ^{||} Alexei Sokolov, ^{||,†}
⁵ and Marian Paluch [‡]

⁶ [†]Institute of Chemistry, University of Silesia, 9 Szkolna Street, 40-006 Katowice, Poland

⁷ [‡]Institute of Physics, University of Silesia, Uniwersytecka 4, 40-007 Katowice, Poland

⁸ SMCEBI, University of Silesia, 75 Pułku Piechoty, 41-500 Chorzów, Poland

⁹ Leibniz Institute for Catalysis, Albert-Einstein-Str. 29a, 18059 Rostock, Germany

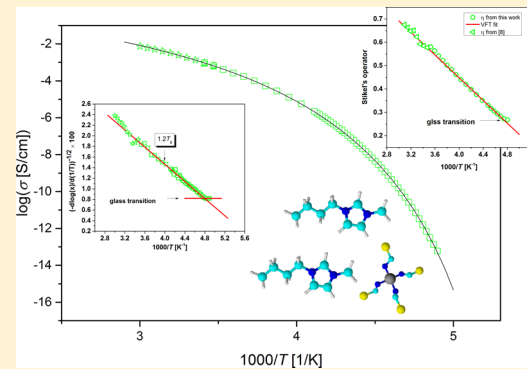
¹⁰ ^{||}Center for Nanophase Materials Sciences, Oak Ridge National Laboratory, Oak Ridge, Tennessee 37831, United States

¹¹ [†]Chemical Sciences Division, Oak Ridge National Laboratory, Oak Ridge, Tennessee 37831, United States

¹² [#]Department of Chemistry, University of Tennessee Knoxville, Knoxville, Tennessee 37996, United States

13 Supporting Information

ABSTRACT: Dynamic crossover above T_g has been recognized as a characteristic feature of molecular dynamics of liquids approaching glass transition. Experimentally, it is manifested as a change in Vogel–Fulcher–Tammann dependence or a breakdown of the Stokes–Einstein and related relations. In this paper, we report the exception from this rather general pattern of behavior. By means of dielectric, ultrasonic, rheological, and calorimetric methods, dynamics of two good ionic conductors $(\text{BMIm})_2[\text{Co}(\text{NCS})_4]$ and $(\text{EMIm})_2[\text{Co}(\text{NCS})_4]$ of less common stoichiometry (2:1) was studied in a very broad temperature range. However, none of the mentioned dynamic changes was observed in the entire studied temperature range. On the contrary, the single VFT and the same fractional Walden coefficient were found for conductivity and viscosity changes over 12 decades. Moreover, ultrasonic studies revealed that the data at temperatures which cover the normal liquid region cannot be fitted by a single exponential decay, and the Cole–Cole function should be used instead.



29 ■ INTRODUCTION

30 Ionic liquids (ILs) have triggered great interest in both science
31 and industry. Their special attraction lies in their unique
32 properties like a huge range of fluidity, chemical and thermal
33 stability, high conductivity ($>10^{-4}$ S·cm⁻¹), or a large
34 electrochemical window together with fast ion mobility, all of
35 which make them especially promising candidates for electro-
36 chemical applications.¹ Furthermore, many of them are
37 nonvolatile and nonflammable, although nowadays it is obvious
38 that these properties are not general.² In addition, their impact
39 on the natural environment is not as neutral as it was thought
40 earlier, although they are still regarded as “green” chemicals.
41 Another branch of industry interested in special properties of
42 ILs is pharmacy.^{3,4}

43 Among different classes of ILs, metal-containing ones attract
44 particular attention of researchers due to properties that cannot
45 be associated with typical ILs.⁵ Unfortunately, the most popular
46 ILs with halogenometalate complexes as anions turn out to be
47 unstable.⁵ A new class of substances are liquids with thio- and
48 isothiocyanatometalates of transition metals in anions.⁶ In the

49 previous papers,^{7,8} few basic properties of newly synthesized
50 paramagnetic 1-alkyl-3-methylimidazolium ionic liquids
51 ($\text{EMIm})_2[\text{Co}(\text{NCS})_4]$ and $(\text{BMIm})_2[\text{Co}(\text{NCS})_4]$) were re-
52 ported. These substances appeared to have many features
53 interesting for engineers.^{7,8} However, their chemical structure,
54 less common stoichiometry (2:1) due to divalent anion, and
55 complex nature of the anion makes them also very interesting
56 from the point of view of basic science. Recently, molecular
57 dynamics of supercooled and glassy ILs have been extensively
58 studied. An in-depth knowledge of molecular dynamics’
59 behavior near T_g of ionic liquids is also necessary to formulate
60 a complete theory of a liquid–glass transition. Thus, we decided
61 to expand the scope of our interests beyond the common
62 physicochemical characteristics of these materials. In this paper,
63 we focused on the molecular dynamics of both mentioned ILs
64 in normal and supercooled liquid as well as in a glassy state.⁶⁴

Received: July 22, 2015

Revised: August 10, 2015

Combining ultrasonic, dielectric, rheological, and calorimetric methods, we were able to trace evolution of dynamical properties of studied samples over 12 decades, down to the glass transition temperature. As a result, we observed several interesting phenomena like non-Newtonian behavior, lack of the dynamical crossover in the range of $1.2-1.5T_g$, and slight decoupling between conductivity and structural relaxation times. Because $(\text{EMIm})_2[\text{Co}(\text{NCS})_4]$ and $(\text{BMIm})_2[\text{Co}(\text{NCS})_4]$ behave differently than commonly noted for ionic liquids, it provides a better understanding of the mechanisms governing molecular dynamics of such type of substances over a very wide temperature range, including the supercooled state.

EXPERIMENTAL SECTION

Ionic liquids investigated $(\text{EMIm})_2[\text{Co}(\text{NCS})_4]$ (I) and $(\text{BMIm})_2[\text{Co}(\text{NCS})_4]$ (II) were synthesized and purified as described in ref 7. All samples were kept under argon, and prior to use, they were additionally degassed by a vacuum pump over 24 h to remove possible traces of solvents and moisture. The water concentration (93.863 ppm for (I) and 132.72 ppm (II)) was checked by Karl Fischer titration.

The ambient pressure, isothermal, frequency dependent dielectric measurements were carried out using a Novo-Control GMBH Alpha Analyzer in a frequency range from 10^{-2} to 10^7 Hz. The sample was placed in a parallel flat stainless steel capacitor. Temperature was controlled by a Novo-Control Quattro system, with a nitrogen gas cryostat. Temperature stability of the sample was better than 0.1 K.

Calorimetric measurements were carried out by Mettler-Toledo DSC apparatus equipped with a liquid nitrogen cooling accessory and a HSS8 ceramic sensor (heat flux sensor with 120 thermocouples) with implemented stochastic temperature-modulated differential scanning calorimetry (TMDSC) method (TOPEM). Temperature and enthalpy calibrations were performed by using indium and zinc standards.

Ultrasound absorption measurements were performed with the use of the homemade apparatus (described in detail in ref 9) working on the standard pulse technique (first traveling pulse and the variable path length). The measurements were performed for some chosen discrete frequencies from range 10 to 300 MHz by means of three pairs of ultrasonic heads at the temperatures (293.15 and 298.15) K and at atmospheric pressure. Temperature (± 0.05 K) was maintained with the thermostat unit. To avoid contact with air, the measuring cell was filled with argon during the measurements.

RESULTS AND DISCUSSION

Generally speaking, the ionic liquids $(\text{EMIm})_2[\text{Co}(\text{NCS})_4]$ (I) and $(\text{BMIm})_2[\text{Co}(\text{NCS})_4]$ (II) are relatively easy to supercool. However, the first one shows some tendency for crystallization, which is in agreement with other imidazole-based ILs.⁵ In this case, a cold crystallization was observed at $T_c = 264$ K with melting point at $T_m = 292$ K when heated with a rate of 5 K/min. The crystallization process does not occur at higher heating rates.

Dielectric spectra were measured in a temperature range from below T_g (208 K for (I) and 209 for (II)) up to 293.15 K for $(\text{BMIm})_2[\text{Co}(\text{NCS})_4]$ and 233.15 K for $(\text{EMIm})_2[\text{Co}(\text{NCS})_4]$. Usually the dielectric data of conducting materials are analyzed in either conductivity or electrical modulus representation. Both representations trace the same phenomena and are interrelated with each other. The results in both

representations are shown in Figure 1a,b and Figure 1c,d for (I) and (II), respectively. In an imaginary part of modulus spectra

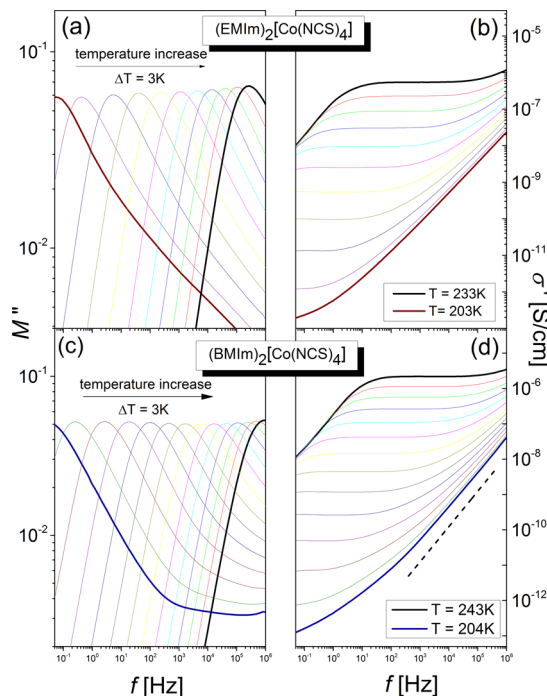


Figure 1. Representative spectra of imaginary part of modulus and real part of conductivity for $(\text{EMIm})_2[\text{Co}(\text{NCS})_4]$ (a,b) and $(\text{BMIm})_2[\text{Co}(\text{NCS})_4]$ (c,d). Dashed line in panel (d) shows the slope equal to 1. The horizontal arrow indicates the direction of the experiment.

(M''), the dominant feature is the asymmetric peak of the σ -relaxation. The inverse of the frequency of M'' peak maximum designates the relaxation time ($\tau_\sigma = (1/2)\pi f_{max}$).

Values of the dc-conductivity at a given temperature can be determined from the plateau region in the middle part of the conductivity spectrum. The temperature dependence of the dc-conductivity, presented in Figure 2, is very similar for both samples, although as expected, values of conductivity of $(\text{EMIm})_2[\text{Co}(\text{NCS})_4]$ are a bit higher due to the fact that shorter side chain makes these cations more mobile. For $(\text{BMIm})_2[\text{Co}(\text{NCS})_4]$, we were able to carry out dielectric measurements in a wider temperature range due to the lack of tendency to crystallization. Analysis of conductivity data obtained for sample (II) reveals unexpected behavior with decreasing temperature. In many fragile liquids (liquids with strongly non-Arrhenius temperature variations of relaxation time), the temperature dependence of relaxation times reveals several characteristic changes: At high temperatures, it follows an Arrhenius law; then at some T_A , it changes to a VFT dependence; and at some T_B between T_A and T_g , it usually crosses over to another VFT. This T_B usually appears in the range of $\sim 1.2-1.5T_g$.¹⁰ The last change of the temperature dependence of relaxation times is observed at T_g where temperature dependence crosses over to an Arrhenius type. Among different views on the origin of the dynamic crossover at T_B , the most common ascribes it a temperature below which cooperativity becomes a crucial factor and where dynamical heterogeneity of the system starts to play a key role in the molecular dynamics.^{11,12} The change of VFT dependence at T_B was observed for small molecular liquids like OTP,¹³ diisobutyl

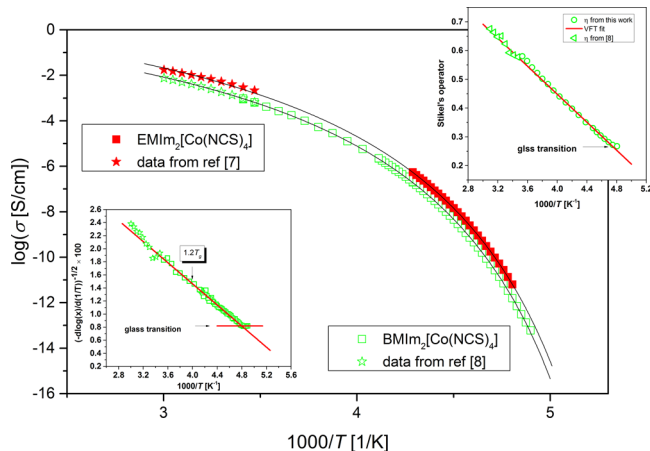


Figure 2. Activation plot of the conductivity above glass transition temperature of $(\text{EMIm})_2[\text{Co}(\text{NCS})_4]$ (solid squares) and $(\text{BMIm})_2[\text{Co}(\text{NCS})_4]$ (open squares). (ψ) and (ξ) data from refs 7 and 8, respectively. Solid lines are fits by means of eq 1 (parameters are given in Table 1 of Supporting Information). Left lower inset: Stickel's analysis for conductivity data of $(\text{BMIm})_2[\text{Co}(\text{NCS})_4]$. Right upper inset: Stickel's analysis for viscosity data of $(\text{BMIm})_2[\text{Co}(\text{NCS})_4]$.

157 phthalate,¹⁴ polymers like polyisoprene,¹⁵ and ionic liquids like
158 (OMIm) (NTf_2).¹⁶

159 Parameter commonly used to characterize quantitatively the
160 departure of the temperature dependence from the Arrhenius
161 behavior at T_g (and the same the fragility of the system) is the
162 so-called steepness index or fragility m defined as $m = (d\log x /$
163 $d(T_g/T))|_{T = T_g}$, where x denotes one of the transport properties
164 like viscosity and conductivity, or structural relaxation times.
165 Fragility was originally derived for viscosity however flexibility
166 in choosing the quantity for which the fragility is defined exists
167 as long as they are correlated with changes of structure. In the
168 case of our samples, fragility determined from the temperature
169 dependence of the viscosity (at T_g taken as T for which $\eta = 10^{10}$
170 $\text{Pa}\cdot\text{s}$) is $m = 93.4$ for sample (I) and $m = 87.5$ for sample (II). It
171 means that both samples are very fragile, and for such systems,
172 T_B was sometimes observed even at such high temperatures as
173 $1.5T_g$.

174 A close examination of Figure 2 reveals that for sample (II),
175 there is a single VFT in a form:

$$x = x_\infty \exp\left(\frac{B}{T - T_0}\right) \quad (1)$$

177 (where x denotes σ – conductivity or η – viscosity, x_∞ is pre-
178 exponential factor, T_0 – temperature of an ideal glass transition
179 and B – a material constant) can perfectly describe the
180 temperature dependence of x in the entire temperature range
181 above T_g . To make our experimental range of temperatures
182 even broader, we added to Figure 2 conductivity data obtained
183 by Geppert-Rybckyńska^{7,8} in a normal liquid state at temper-
184 atures as high as 333 K, which is around $1.6T_g$.

185 The best way to identify precisely the existence of any
186 specific changes in temperature dependence of the interested
187 transport coefficient is to analyze the experimental data by
188 means of the so-called Stickel's derivative operators.¹⁷ These
189 operators linearize VFT (equation 1) and transform the
190 Arrhenius relation

$$x = x_\infty \exp\left(\frac{-E_a}{RT}\right) \quad (2)$$

191 into a constant value according to the following equation (in
192 the case of Arrhenius relation $T_0 = 0$):
193

$$[\text{dlog}(x)/\text{d}(1/T)]^{-1/2} = (B)^{-1/2} \cdot (1 - T_0/T) \quad (3)$$

195 where x is the studied property, B – a respective constant.
196 Thus, any change in the temperature dependence of x should
197 be visible as an intersection of straight lines. The result of such
198 analysis for $(\text{BMIm})_2[\text{Co}(\text{NCS})_4]$ is presented in the inset in
199 Figure 2. It clearly shows that the only visible crossover occurs
200 around 209 K and is related to crossing the glass transition. On
201 the other hand, no clear indication of existence of T_B exists up
202 to $1.6T_g$. However, one can note a slight deviation from the line
203 obtained for Stickel's operator applied to VFT fit at the high
204 temperature limit of the conductivity data (see lower left inset
205 to Figure 2). It is not possible to settle whether it is an
206 indication of a very slight crossover in this range of
207 temperatures or just scatter of the data. On the one hand,
208 the deviation from the straight line obtained from VFT fit is
209 within the upper limit of allowed deviation (basing on a 4d
210 test). On the other hand, systematic trend of this deviation may
211 indicate the real change in this dependence. More conclusive
212 picture can be obtained for viscosity. Result of Stickel's analysis
213 for viscosity data of (II) is shown in upper right inset of Figure
214 2. Again, when we add the data from ref 8, no signs of the
215 dynamical crossover can be found at any temperature up to 323
216 K $\sim 1.55T_g$. It is worth mentioning that the same pattern of
217 behavior was previously found for $(\text{BMIm})[\text{PF}_6]$, $(\text{BMIm})-$
218 $[\text{NTf}_2]$ and $(\text{BMIm})[\text{TFA}]$,¹⁸ for which temperature depend-
219 ence of structural relaxation times and diffusion coefficient were
220 studied. The question arises immediately whether it can be
221 more general behavior of ILs or at least for BMIm-based
222 samples. In this context, it has to be noted that all the ILs
223 studied by Griffin¹⁸ contained BMIm cation similarly to our
224 sample. It is interesting that one of the very few known
225 molecular liquids for which T_B is not observed is di-*n*-butyl
226 phthalate. It turns out that structure of di-*n*-butyl phthalate¹⁴
227 slightly resembles BMIm cation. Thus, their behavior may also
228 be similar. The influence of the cation structure on the position
229 of the temperature at which studied crossover occurs become
230 more visible when one takes into account the recent
231 observation for (OMIm) (NTf_2) for which the dynamic
232 crossover at T_B was recently found.¹⁶ In this respect, it is also
233 interesting to note that the lack of VFT change in a common
234 temperature range for BMIm-based ILs is insensitive to the
235 different stoichiometry of our ILs (2:1) caused by bivalency of
236 the anion.

237 Although change in the VFT dependence is the best known
238 sign of the studied crossover, often it is treated as a
239 nonsufficient condition. It is a long-standing discussion on
240 the validity of the VFT-equation fits of the data obtained at a
241 very broad temperature range. Therefore, in parallel, other
242 parameters are studied that can prove the existence/
243 nonexistence of the dynamic crossover.
244

245 Temperature dependence of σ -relaxation times are presented
246 in Figure 3a and b for (I) and (II), respectively. It is commonly
247 believed that for ILs, temperature dependence of σ and τ_σ
248 follows that of shear viscosity η , as expected from the Walden
249 rule for conductivity in molecular liquids. However, it was
250 shown for several ionic materials that there is a decoupling
251 between viscosity (structural relaxation) and conductivity

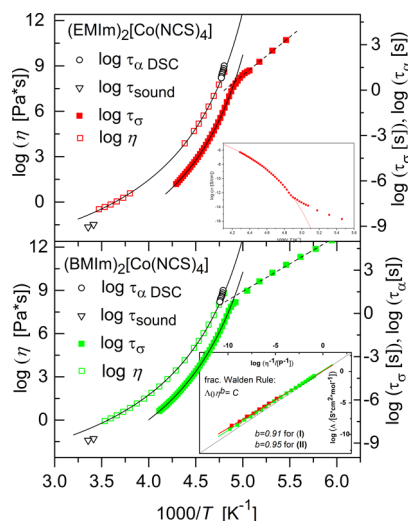


Figure 3. Relaxation map of (a) $(\text{EMIm})_2[\text{Co}(\text{NCS})_4]$ and (b) $(\text{BMIm})_2[\text{Co}(\text{NCS})_4]$. Conductivity relaxation times are compared with viscosity and structural relaxation times from TMDSC. At the highest temperature limit, relaxation times obtained from ultrasound absorption are added. Solid and dashed lines are VFT and Arrhenius fits, respectively. Crossover point on $\tau_\sigma(T)$ dependence determines T_g . Upper inset: dc-conductivity vs inverse temperature with clearly visible crossover from the VFT to Arrhenius dependence. Lower inset: Walden plot.

251 (conductivity relaxation). It is especially prominent for protic
252 ionic liquids¹⁹ due to enhanced proton conduction caused by
253 Grotthuss mechanism.

254 In Figure 3, glass transition is demonstrated as a crossover
255 from VFT (eq 1) to Arrhenius (equation 2) temperature
256 dependence of σ -relaxation times. Because the same crossover
257 is visible on the temperature dependence of the data of dc-
258 conductivity (see inset to Figure 3a), such a change is a physical
259 phenomenon not an artifact resulting from application of
260 Modulus representation. In fact, this effect has been observed
261 for some other ionic liquids.^{3,20} On the other hand, there are
262 also examples of ionic liquids for which no decoupling between
263 dc-conductivity and viscosity or diffusion coefficient is observed
264 down to glass transition temperature. Among them are liquids
265 with cations based on imidazole.^{21,22} We compared these data
266 with the viscosity and specific heat relaxation, which reflect the
267 structural relaxation. As shown in Figure 3, inflection occurs at
268 a temperature for which structural relaxation reaches 1000 s.
269 Usually, these are conditions given for the glass transition.
270 However, one has to be aware that at this temperature,
271 conductivity relaxation times do not reach the same value. The
272 crossover from VFT to Arrhenius-type behavior can be found
273 around 10 s for (II) and 1 s for (I). It means that there is a
274 decoupling between conductivity and structural relaxation. It is
275 very interesting that such decoupling was not observed for
276 structurally very similar IL $(\text{BMIm})[\text{BF}_4]$.²³ It means that in
277 this case, the anion must play an important role. The
278 phenomenon of decoupling between studied properties is
279 also clearly visible in the inset to Figure 3, in violation of the
280 classical Walden rule. Instead, fractional Walden rule ($\Lambda_0 \eta^b =$
281 const) can be used, where b is a measure of decoupling. In our
282 case, b values equal 0.91 and 0.95 for samples (I) and (II),
283 respectively (see the inset in Figure 3). The decoupling of
284 diffusion and structural relaxation (viscosity) has been found in
285 many glass forming liquids, but usually only for temperatures

below T_g .²⁴ For our samples, almost the same values of the
286 exponent b were obtained in the entire temperature range. This
287 observation strengthens our view that no change in the
288 dynamics occurs in the range of 1.2 – $1.5T_g$. If any crossover
289 exists for this sample, it occurs above $1.5T_g$.

290 Further interesting details can be revealed from studies of the
291 ultrasound absorption in normal liquid range. The ultrasound
292 absorption coefficient α per squared frequency f (i.e. the
293 product $\alpha \cdot f^{-2}$) for both liquids are summarized in Table 2 of
294 Supporting Information. As evidenced from this table and
295 Figure 4a,b, the dependence of the quotient $\alpha \cdot f^{-2}$ on frequency
296 f4

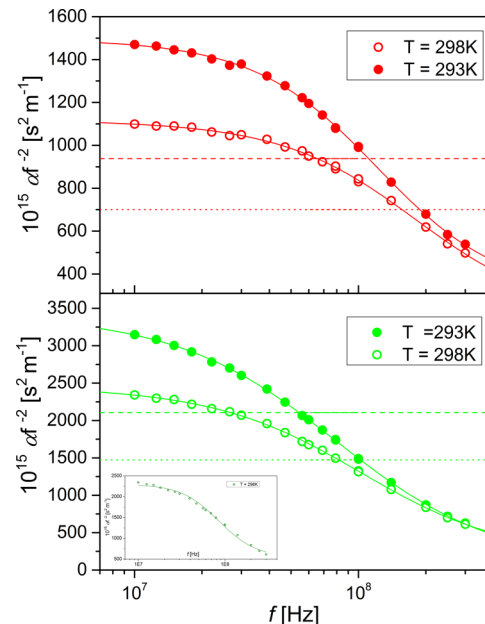


Figure 4. Ultrasound absorption coefficient per squared frequency $\alpha \cdot f^{-2}$ versus $\log f$ for (upper panel) $(\text{EMIm})_2[\text{Co}(\text{NCS})_4]$ and (lower panel) $(\text{BMIm})_2[\text{Co}(\text{NCS})_4]$ at temperatures of 293.15 K (●) and 298.15 K (○). Solid lines are fits by means of CC function. Dashed and dotted lines—classical absorption at temperatures 293.15 and 298.15 K, respectively. The inset presents the fit with use of a single Debye function to ultrasonic spectrum for $(\text{BMIm})_2[\text{Co}(\text{NCS})_4]$ at 298.15 K.

297 changes strongly with temperature. It appears also that within
298 the investigated frequency range the quotient $\alpha \cdot f^{-2}$ is clearly
299 dependent on frequency as high as above 10 MHz. Thus, in
300 both cases, the dispersion characteristics $d(\alpha \cdot f^{-2})/df < 0$ is
301 observed. Moreover, both liquids are rather highly absorbing;
302 that is, the frequency normalized attenuation values (at $T =$
303 298.15 K and $f = 100$ MHz) are 837×10^{-15} and 1321×10^{-15}
304 $\text{s}^2 \cdot \text{m}^{-1}$, respectively. At the same time, it is observed in both
305 liquids that above some frequency, the experimental values of
306 $\alpha \cdot f^{-2}$ are smaller than those predicted by the Navier–Stokes
307 relation (α_{cl}). In other words, the absorption curves shown in
308 Figure 4 indicate that $\alpha > \alpha_{\text{cl}}$ at lower frequencies and $\alpha < \alpha_{\text{cl}}$ at
309 higher frequencies, and the curves also demonstrate that the
310 frequency for which $\alpha = \alpha_{\text{cl}}$ decreases with increasing
311 temperature. Most probably, this kind of behavior results
312 from a relaxation mechanism of the viscous type. Similar
313 behavior has been reported previously for several molecular
314 liquids, including 1-dodecanol²⁵ and castor oil,²⁶ diols²⁷ as well
315 as ionic liquids (OMIm) (NTf_2)²⁸ and a series of (C_nMIm)
316 (PF_6).²⁹ The obtained numerical values of $\alpha_{\text{cl}} \cdot f^{-2}$ are

317 summarized in Table 3 of the [Supporting Information](#). Shear
318 viscosity used for calculations were taken from refs 7,8.

319 The small ratio of the observed absorption to that calculated
320 from the Stokes rule (i.e., classical absorption) and the negative
321 temperature coefficients of the experimental absorption in the
322 nondispersing region are observed for both liquids. These
323 findings are characteristic for liquids with structural relaxation
324 (i.e., for liquids from group III according to liquid classification
325 in relation to absorption data).³⁰ Detailed inspection of Table 3
326 shows that for (I), α/α_{cl} is temperature independent. This
327 finding indicates an equal temperature dependence of the
328 volume viscosity, η_V , and shear viscosity. On the other hand, for
329 (II), this ratio decreases with temperature. A similar scenario
330 was observed in the case of (EMIm) and (OMIm) (NTf₂).²⁸ It
331 means that changes in the alkyl chain cause the detectable
332 differences in molecular mechanisms of the volume and shear
333 viscosity. However, in the case of (OMIm) cation, the
334 temperature dependence was weaker in comparison to that
335 observed for (II). Immediately, the question arises as to
336 whether it is anion dependent. Another possible scenario is that
337 there is a maximum of difference for cations with alkyl
338 substituent between C₂ and C₈ beyond which again the
339 molecular mechanisms of the volume and shear viscosity
340 become similar.

341 From the frequency-dependent ultrasonic absorption data,
342 relaxation times can be obtained via the following relation:

$$\alpha \cdot f^{-2} = \sum_{i=1}^n A_i \cdot (1 + (f/f_{i,rel})^2)^{-1} + B \quad (5)$$

344 where A_i and $f_{i,rel}$ are the relaxation amplitudes and relaxation
345 frequencies, respectively. B represents the sum of the classical
346 part of absorption and contributions from processes with
347 relaxation frequencies considerably higher than $f_{i,rel}$. It appears
348 that for the studied liquids, the frequency dependence of
349 ultrasonic absorption data cannot be fitted with a single Debye-
350 type relaxation processes ($n = 1$). It is in odd to what is
351 commonly observed for ultrasonic spectra of both molecular
352 and ionic liquids in a normal liquid regime.^{27,28} Thus, in this
353 paper, we would like to discuss fitting with a stretched function
354 (shape parameters (α and β) should be introduced to [eq 5](#)).
355 We found that not a Cole-Davidson but a symmetrical Cole-
356 Cole function with the shape parameter (α_{CC}) around 0.8
357 provides the best fit (full results are given in a Table 4 of a
358 [Supporting Information](#)). The relaxation times denoted as τ
359 sound (calculated as $\tau_{rel} = (2 \cdot \pi \cdot f_{rel})^{-1}$) can be found in [Figure 3](#).
360 Ultrasonic results are very interesting for two reasons. First,
361 stretching of this spectrum again proves that in the temper-
362 atures for which the spectra were taken, we are in the region
363 which we can call a complex liquid regime. Otherwise, one
364 single Debye relaxation should be observed. Moreover, the
365 symmetrical shape of the spectra is puzzling. A possible
366 explanation is that the process which can be observed by the
367 ultrasonic method does not reveal features of the α relaxation
368 but of the β -one. In fact, it was reported several times that in
369 shear mechanical spectra, the amplitude of the β -process at low
370 temperatures far exceeds the one observed for dielectric
371 spectra.³¹ Moreover, it increases much faster with temper-
372 ature.³² Thus, it is very likely that for such high frequencies as
373 used in the ultrasonic method, it is the dominant relaxation
374 process. In such case, our samples would be examples of
375 scenario I according to Donth and co-workers.³³ It also explains
376 why the relaxation times obtained from the ultrasonic

377 experiment does not fully agree with the rest of the data (see
378 [Figure 3](#)). If we take into account the Donth's scenario I,
379 known the best for the PMMA, it is probable that in our case,
380 low amplitude, slower alpha relaxation is buried beneath the
381 lower frequency side of the clearly observed β -process. As
382 mentioned above, there are examples for both single Debye and
383 stretched shape of the ultrasonic spectra in the literature; it
384 would be very interesting to determine whether these
385 observations always correlate with the position of T_B for the
386 studied materials, which seems to be very likely on the basis of
387 our data.

CONCLUSIONS

388 Imidazole-based cations are known for their ability to form
389 quite effective H-bonding systems. However, with the
390 elongation of the alkyl chain, the influence of the nonpolar
391 domains increases, and the C2 atom involved in H-bonds with
392 sulfur atom of the anion^{34,35} becomes less acidic. This probably
393 causes higher decoupling in sample (I) (due to contribution
394 from protonic conduction) and differences in ultrasound
395 absorption. On the other hand, it is not fully understood
396 whether sterical hindrance, various types of interactions
397 (Coulomb interactions, H-bonds) between cations and anions
398 or non-Newtonian nature of studied liquids are the reasons why
399 the dynamical crossover with all accompanying phenomena is
400 not observed in the region of 1.2–1.5 T_g . In fact, it remains an
401 open question whether the observations (lack of change in VFT
402 dependence at T_B , lack of the point in which Walden rule
403 breaks down, and symmetrically stretched ultrasonic absorption
404 spectra in the fluid regime) are related to each other and
405 whether each of them indeed can be treated as an indicator for
406 existence/nonexistence of a dynamical crossover. However, all
407 our experimental data seem to indicate that the dynamical
408 heterogeneity and cooperativity play the same role in the
409 molecular dynamics of ionic liquids studied herein in the
410 vicinity of T_g as it does in normal liquid state at least up to 1.5–
411 1.6 T_g . It means that even at temperatures much higher than T_g
412 they behave like supercooled liquids and not like normal
413 liquids.

414 More experimental data in broad temperature range are
415 necessary to answer the question whether it is a general rule for
416 ILs or it is only specific feature of samples based on BMIIm
417 cation.

ASSOCIATED CONTENT

Supporting Information

421 The Supporting Information is available free of charge on the
422 ACS Publications website at DOI: [10.1021/acs.jpcc.5b07123](https://doi.org/10.1021/acs.jpcc.5b07123).

423 Contains Tables 1–4 according to description given in
424 text ([PDF](#))

AUTHOR INFORMATION

Corresponding Author

426 *E-mail: stella.hensel-bielowka@us.edu.pl.

Notes

428 The authors declare no competing financial interest.

ACKNOWLEDGMENTS

430 The authors S.H-B., Z.W., K.G., and M.P. are grateful for the
431 financial support by the National Science Centre within the
432 framework of the Opus project (grant no. DEC-2011/03/B/

434 ST3/02072). A.S. and Y.W. acknowledge financial support
 435 from NSF under the grant CHE-1213444.

436 ■ REFERENCES

- 437 (1) Rooney, D.; Jacquemin, J.; Gardas, R. Thermophysical Properties
 438 of Ionic Liquids. *Top Curr. Chem.* **2009**, *290*, 185–212.
- 439 (2) Wellens, S.; Thijss, B.; Binnemans, K. How Safe are Protic Ionic
 440 Liquids? Explosion of Pyrrolidinium Nitrate. *Green Chem.* **2013**, *15*,
 441 3484–3485.
- 442 (3) Wojnarowska, Z.; Grzybowska, K.; Hawelek, L.; Swiety-Pospiech,
 443 A.; Masiewicz, E.; Paluch, M.; Sawicki, W.; Chmielewska, A.; Bujak, P.;
 444 Markowski, J. Molecular Dynamics Studies on the Water Mixtures of
 445 Pharmaceutically Important Ionic Liquid Lidocaine HCl. *Mol. Pharmaceutics* **2012**, *9*, 1250–1261.
- 446 (4) Stoimenovski, J.; Dean, P. M.; Izgorodina, E. I.; MacFarlane, D.
 447 Protic Pharmaceutical Ionic Liquids and Solids: Aspects of Protonics.
 448 *Faraday Discuss.* **2012**, *154*, 335–352.
- 449 (5) Yoshida, Y.; Saito, G. Influence of Structural Variations in 1-
 450 Alkyl-3-methylimidazolium Cation and Tetrahalogenoferrate (III)
 451 Anion on the Physical Properties of the Paramagnetic Ionic Liquids.
 452 *J. Mater. Chem.* **2006**, *16*, 1254–1262.
- 453 (6) Nockemann, P.; Thijss, B.; Postelmans, N.; Van Hecke, K.; Van
 454 Meervelt, L.; Binnemans, K. Anionic Rare-Earth Thiocyanate
 455 Complexes as Building Blocks for Low-Melting Metal-Containing
 456 Ionic Liquids. *J. Am. Chem. Soc.* **2006**, *128*, 13658–13659.
- 457 (7) Peppel, T.; Kockerling, M.; Geppert-Rybczyńska, M.; Ralys, R.
 458 V.; Lehmann, J. K.; Verevkin, S. P.; Heintz, A. Low-Viscosity
 459 Paramagnetic Ionic Liquids with Doubly Charged $[\text{Co}(\text{NCS})_4]^{2-}$
 460 Ions. *Angew. Chem., Int. Ed.* **2010**, *49*, 7116–7119.
- 461 (8) Geppert-Rybczyńska, M.; Lehmann, J. K.; Peppel, T.; Kockerling,
 462 M.; Heintz, A. Studies of Physicochemical and Thermodynamic
 463 Properties of the Paramagnetic 1-Alkyl-3-methyl- imidazolium Ionic
 464 Liquids $(\text{EMIm})_2[\text{Co}(\text{NCS})_4]$ and $(\text{BMIm})_2[\text{Co}(\text{NCS})_4]$. *J. Chem.*
 465 *Eng. Data* **2010**, *55*, 5534–5538.
- 466 (9) Zorębski, E.; Zorębski, M.; Gepert, M. Ultrasonics Absorption
 467 Measurements by Means of a Megahertz – Range Measuring Set. *J.
 468 Phys. IV* **2006**, *137*, 231–235.
- 469 (10) Novikov, V. N.; Sokolov, A. P. Universality of the Dynamic
 470 Crossover in Glass-Forming Liquids: A “Magic” Relaxation Time. *Phys.
 471 Rev. E: Stat. Phys., Plasmas, Fluids, Relat. Interdiscip. Top.* **2003**, *67*,
 472 031507.
- 473 (11) Casalini, R.; Roland, C. M. Scaling of the Supercooled Dynamics
 474 and Its Relation to the Pressure Dependences of the Dynamic
 475 Crossover and the Fragility of Glass Formers. *Phys. Rev. B: Condens.
 476 Matter Mater. Phys.* **2005**, *71*, 014210.
- 477 (12) Ngai, K. L. *Relaxation and Diffusion in Complex Systems*; Springer
 478 Science + Business Media LLC: New York, 2011.
- 479 (13) Hansen, C.; Stickel, F.; Berger, T.; Richert, R.; Fischer, E. W.
 480 Dynamics of Glass-Forming Liquids. III. Comparing the Dielectric α -
 481 and β -Relaxation of 1-propanol and o-terphenyl. *J. Chem. Phys.* **1997**,
 482 107, 1086–1093.
- 483 (14) Sekula, M.; Pawlus, S.; Hensel-Bielowka, S.; Ziolo, J.; Paluch,
 484 M.; Roland, C. M. Structural and Secondary Relaxations in
 485 Supercooled Di-n-butyl Phthalate and Diisobutyl Phthalate at Elevated
 486 Pressure. *J. Phys. Chem. B* **2004**, *108*, 4997–5003.
- 487 (15) Pawlus, S.; Kunal, K.; Hong, L.; Sokolov, A. P. Influence of
 488 Molecular Weight on Dynamic Crossover Temperature in Linear
 489 Polymers. *Polymer* **2008**, *49*, 2918–2923.
- 490 (16) Paluch, M.; Wojnarowska, Z.; Goodrich, P.; Jacquemin, J.;
 491 Pionteck, J.; Hensel-Bielowka, S. Can the Scaling Behavior of Electric
 492 Conductivity be Used to Probe the Self-Organizational Changes in
 493 Solution with Respect to the Ionic Liquid Structure? The Case of
 494 $[\text{C}8\text{MIM}][\text{NTf}_2]$. *Soft Matter* **2015**, *11*, 6520.
- 495 (17) Stickel, F.; Fischer, E. W.; Richert, R. Dynamics of Glass-
 496 Forming Liquids. I. Temperature-Derivative Analysis of Dielectric
 497 Relaxation Data. *J. Chem. Phys.* **1995**, *102*, 6251–6257.
- 498 (18) Griffin, P.; Agapov, A.; Sokolov, A. Translation-Rotation
 499 Decoupling and Nonexponentiality in Room Temperature Ionic
 500 Liquids. *Phys. Rev. E* **2012**, *86*, 021508.
- 501 (19) Swiety-Pospiech, A.; Wojnarowska, Z.; Pionteck, J.; Pawlus, S.;
 502 Grzybowski, A.; Hensel-Bielowka, S.; Grzybowska, K.; Szulc, A.;
 503 Paluch, M. High Pressure Study of Molecular Dynamics of Protic Ionic
 504 Liquid Lidocaine Hydrochloride. *J. Chem. Phys.* **2012**, *136*, 224501.
- 505 (20) Rivera, A.; Brodin, A.; Pugachev, A.; Rössler, E. A. Orientational
 506 and Translational Dynamics in Room Temperature Ionic Liquids. *J. Chem. Phys.* **2007**, *126*, 114503.
- 507 (21) Sangoro, J. R.; Kremer, F. Charge Transport and Glassy
 508 Dynamics in Ionic Liquids. *Acc. Chem. Res.* **2012**, *45*, 525–532.
- 509 (22) Sangoro, J. R.; Iacob, C.; Naumov, S.; Valiullin, R.; Rexhausen,
 510 H.; Hunger, J.; Buchner, R.; Strehmel, V.; Karger, J.; Kremer, F. Diffusion
 511 in Ionic Liquids: the Interplay Between Molecular Structure and
 512 Dynamics. *Soft Matter* **2011**, *7*, 1678–1681.
- 513 (23) Sangoro, J. R.; Iacob, C.; Serghei, A.; Naumov, S.; Galvosas, P.;
 514 Karger, J.; Wespe, C.; Bordusa, F.; Stoppa, A.; Hunger, J.; Buchner, R.;
 515 Kremer, F. Electrical Conductivity and Translational Diffusion in the
 516 1-Butyl-3-methylimidazolium Tetrafluoroborate Ionic Liquid. *J. Chem. Phys.* **2008**, *128*, 214509.
- 517 (24) Pawlus, S.; Paluch, M.; Sekula, M.; Ngai, K. L.; Rzoska, S. J.;
 518 Ziolo, J. Changes in Dynamic Crossover with Temperature and
 519 Pressure in Glass-Forming Diethyl Phthalate. *Phys. Rev. E: Stat. Phys.,
 520 Plasmas, Fluids, Relat. Interdiscip. Top.* **2003**, *68*, 021503.
- 521 (25) Behrends, R.; Kaatze, U. Hydrogen Bonding and Chain
 522 Conformational Isomerization of Alcohols Probed by Ultrasonic
 523 Absorption and Shear Impedance Spectrometry. *J. Phys. Chem. A* **2001**, *105*,
 524 5829–5835.
- 525 (26) Wuensch, B. J.; Hueter, T. F.; Cohen, M. S. Ultrasonic
 526 Absorption in Castor Oil: Deviations from Classical Behavior. *J. Acoust. Soc. Am.* **1956**, *28*, 311–312.
- 527 (27) Zorębski, E.; Zorębski, M. A Comparative Ultrasonic Relaxation
 528 Study of Lower Vicinal and Terminal Alkanediols at 298.15 K in
 529 Relation to Their Molecular Structure and Hydrogen Bonding. *J. Phys. Chem. B* **2014**, *118*, 5934–5942.
- 530 (28) Zorębski, E.; Geppert-Rybczyńska, M.; Zorębski, M. Acoustics
 531 as a Tool for Better Characterization of Ionic Liquids: A Comparative
 532 Study of 1-Alkyl-3-methylimidazolium Bis[(trifluoromethyl)sulfonyl]-
 533 imide Room-Temperature Ionic Liquids. *J. Phys. Chem. B* **2013**, *117*,
 534 3867–3876.
- 535 (29) Makino, W.; Kishikawa, R.; Mizoshiri, M.; Takeda, S.; Yao, M.
 536 Viscoelastic Properties of Room Temperature Ionic Liquids. *J. Chem. Phys.* **2008**, *129*, 104510.
- 537 (30) Bhatia, A. B. *Ultrasonic Absorption: An Introduction to the Theory
 538 of Sound Absorption and Dispersion in Gases, Liquids and Solids*;
 539 Clarendon Press: Oxford, U.K., 1967.
- 540 (31) Jakobsen, B.; Niss, K.; Maggi, C.; Olsen, N. B.; Christensen, T.;
 541 Dyre, J. C. Beta Relaxation in the Shear Mechanics of Viscous Liquids:
 542 Phenomenology and Network Modeling of the Alpha - Beta Merging
 543 Region. *J. Non-Cryst. Solids* **2011**, *357*, 267–273.
- 544 (32) Jakobsen, B.; Niss, K.; Maggi, C.; Olsen, N. B. Dielectric and
 545 Shear Mechanical Alpha and Beta Relaxations in Seven Glass-Forming
 546 Liquids. *J. Chem. Phys.* **2005**, *123*, 234511.
- 547 (33) Kahle, S.; Schroter, K.; Hempel, E.; Donth, E. Calorimetric
 548 Indications of a Cooperativity Onset in the Crossover Region of
 549 Dynamic Glass Transition for Benzoin Isobutylether. *J. Chem. Phys.* **1999**, *111*,
 550 6462–6470 and the references within..
- 551 (34) Fumino, K.; Wulf, A.; Ludwig, P. The Potential Role of
 552 Hydrogen Bonding in Aprotic and Protic Ionic Liquids. *Phys. Chem. Chem. Phys.* **2009**, *11*,
 553 8790–8794.
- 554 (35) Weingartner, H. Understanding Ionic Liquids at the Molecular
 555 Level: Facts, Problems, and Controversies. *Angew. Chem., Int. Ed.* **2008**, *47*,
 556 654–670.